J Mater Sci: Mater Med (2010) 21:1921–1926
DOI 10.1007/s10856-010-4042-4

Hydroxyapatite formation on porous ceramics of alpha-tricalcium phosphate in a simulated body fluid

Tomohiro Uchino · Kohei Yamaguchi · Ichiro Suzuki · Masanobu Kamitakahara · Makoto Otsuka · Chikara Ohtsuki

Received: 30 August 2009 / Accepted: 1 March 2010 / Published online: 12 March 2010

Abstract Alpha-tricalcium phosphate (α-TCP) ceramic is a bioresorbable material that degrades in bone tissue after implantation, since it exhibits higher solubility than beta-tricalcium phosphate (β-TCP) ceramics. The high solubility of α-TCP in an aqueous solution causes its transformation into hydroxyapatite (HAp) through hydrolysis. While one expects the formation of hydroxyapatite after exposure to an aqueous solution mimicking a body environment, we occasionally find variation in HAp formation in the simulated body fluid (SBF). In the present study, HAp formation resulting from exposure to SBF was investigated for some types of α-TCP ceramics with different porosities and specific surface area. Reduced porosity and large surface area of porous specimens may increase the local density of Ca^{2+} in the surrounding SBF to increase the degree of supersaturation with respect to HAp. Thus, the porosity and specific surface area are significant parameters for determining not only bioabsorbability but also the ability to form HAp.

T. Uchino (✉) · M. Otsuka
Research Institute of Pharmaceutical Sciences, Musashino University, 1-1-20 Shinmachi, Nishitokyo-shi, Tokyo 202-8585, Japan
e-mail: t_uchino@musashino-u.ac.jp

K. Yamaguchi · I. Suzuki · C. Ohtsuki
Graduate School of Engineering, Nagoya University, Furo-cho, Chikusa-ku, Nagoya 464-8603, Japan

M. Kamitakahara
Graduate School of Environmental Studies, Tohoku University, 6-6-20 Aoba, Aramaki, Aoba-ku, Sendai 980-8579, Japan

1 Introduction

Tricalcium phosphate (TCP) is an inorganic compound that produces bioresorbable ceramics for repairing bone tissue. Bioresorbable ceramics are promising candidates for biomaterials showing biodegradability though bone remodeling as well as high biological affinity allowing direct contacts with living bone. There are typically two crystalline phases of tricalcium phosphate, the alpha-phase (α-TCP) and the beta-phase (β-TCP). β-TCP ceramics are used as bioresorbable bone substitutes, while α-TCP powders are the main component of bioactive pastes used as bone fillers called calcium phosphate cement [1–4]. α-TCP is thermodynamically stable at above 1100°C while β-TCP is stable below 1100°C. The solubility of α-TCP is higher than that of β-TCP, which leads to a higher rate of degradation. The high solubility of α-TCP is desirable for a scaffold in drug releasing systems. Recently, Kitamura and his colleagues developed porous α-TCP ceramics with continuous pores of about 1050 μm by a conventional sintering processing [5, 6]. Porous α-TCP ceramics were easily degraded after implantation in bony defects. Because of the high solubility of α-TCP, no agreement has yet been reached on the behavior of α-TCP ceramics in the body environment.

To predict the potential of osteoconduction by in vitro examination, Kokubo and his colleagues propose a simulated body fluid (SBF) with ion concentrations similar to those of human blood plasma [7–10]. Because HAp formation on the surface of ceramics depends on the dissolution of the ceramics, one may expect that α-TCP leads to better HAp formation than β-TCP after exposure to SBF. However, we recently found that HAp formation is rarely observed on the surface of porous α-TCP ceramics with 80% porosity [11]. Therefore, the phenomenon of HAp formation on TCP ceramics in the body environment is still

debatable. We hypothesize that HAp formation on α-TCP ceramics depends on the microstructure and is governed by differences in porosity and the structure of the pores. In the present study, we examined HAp formation on α-TCP ceramics with different porosities and specific surface areas (S.S.A.) after exposure to SBF.

2 Experimental procedure

2.1 Preparation of α-TCP porous ceramics

Specimens of α-TCP with different porosities and S.S.A. were prepared in accordance with previous studies as follows [8, 9]. α-TCP or β-TCP powder and potato starch or rice starch were mixed at various mass ratios. The α-TCP powder was kindly supplied by Taihei Chemical Industrial Co., Ltd., Osaka. The β-TCP powder and potato starch were bought from Nacalai Tesque, Inc., Kyoto, Japan. The rice starch was bought from Sigma-Aldrich, Inc., USA. Distilled water was then added to the powder mixture. The mixture obtained was stirred by a mixer (HM-500 hybrid mixer, Keyence, Japan) for 10 min. The slurry obtained was impregnated in a polyurethane sponge (HR-08, Bridgestone Corporation, Japan) of 15 × 15 × 15 mm^3 with continuous pores 1500 μm in diameter. The specimens were dried at 100°C for 1 h. They were then sintered with different sintering programs depending on the material, and cooled to room temperature at the natural cooling rate of the furnace. Table 1 shows the details of the fabrication including the sintering program. The surfaces of the fabricated porous bodies were characterized by scanning electron microscopy (SEM: JSM-5600, JEOL, Japan) and X-ray diffraction (XRD: RINT2100, Rigaku, Japan). The apparent density of the sintered bodies was measured to determine the relative densities through a calculation based on a theoretical density for α-TCP of 2.86 [12]. The porosities of the specimens were calculated from the relative densities. The S.S.A. values of the specimens were measured by an apparatus based on BET theory (Chem-BET-3000, Yuasa Ionics, Japan).

2.2 Soaking in a simulated body fluid

SBF was prepared by dissolving reagent grade NaCl, $NaHCO_3$, $K_2HPO_4{\cdot}3H_2O$, $MgCl_2{\cdot}6H_2O$, $CaCl_2$, and Na_2SO_4 (Nacalai Tesque, Inc., Japan) in ultra-pure water; Table 2 gives the detailed composition compared with human blood plasma. The solution was buffered at pH 7.25 with an appropriate amount of tris(hydroxymethyl)aminomethane ($(CH_2OH)_3CNH_2$, Nacalai Tesque, Inc., Japan) and HCl at 36.5°C. Rectangular specimens 10 × 10 × 5 mm^3 in size were cut from the obtained porous body with water. These samples were then sonicated for 10 min twice and for 5 min in ethanol. They were dried at 100°C overnight and then soaked in 30 cm^3 of SBF at pH 7.25 and 36.5°C for up to 7 days. They were then taken out of the fluid and gently rinsed with water and ethanol. Finally, they were dried at 100°C overnight. The surfaces of the samples after soaking in SBF were characterized using SEM and XRD. Changes in the calcium (Ca) and phosphorus (P) concentrations of SBF before and after immersion of the specimens were measured by inductively coupled plasma atomic emission spectroscopy (ICP-AES: Optima 2000, PerkinElmer, Germany). Three specimens were tested for each porous body. Error bars show the standard deviations for each condition.

Table 2 Ion concentrations of human blood plasma and simulated body fluid (SBF)

Ion	Concentration (mol m^{-3})	
	Plasma	SBF
Na^+	142.0	142.0
K^+	5.0	5.0
Mg^{2+}	1.5	1.5
Ca^{2+}	2.5	2.5
Cl^-	103.0	147.8
HCO_3^-	27.0	4.2
HPO_4^{2-}	1.0	1.0
SO_4^{2-}	0.5	0.5

Table 1 Fabrication detail of porous specimens

Number	Material	Material mass (g)	Pore former	Pore former mass (g)	Water mass (g)	Sintering program
1	β-TCP	95	Potato starch	5	85	1000°C 3 h, 1400°C 12 h
2	β-TCP	90	Potato starch	10	80	1000°C 3 h, 1400°C 12 h
3	β-TCP	70	Potato starch	30	75	1000°C 3 h, 1400°C 12 h
4	β-TCP	50	Potato starch	50	70	1000°C 3 h, 1400°C 12 h
5	β-TCP	70	Rice starch	30	70	1000°C 3 h, 1400°C 12 h
6	α-TCP	70	Potato starch	30	70	1400°C 12 h
7	α-TCP	50	Potato starch	50	75	1400°C 12 h

3 Results

In the XRD patterns, all the peaks of the fabricated samples were assigned to α-TCP. The fabricated porous ceramics have porosities of 53 to 75% and 0.20 to 0.51 m^2g^{-1} S.S.A. In what follows, specimens with X% porosity and Ym^2g^{-1} S.S.A. are labeled PXAY. Table 3 shows the porosity, S.S.A., and sample name of the α-TCP porous specimens. The porosity of the specimen increased as the ratio of potato starch to TCP powder increased. The S.S.A. of the specimen was controlled by changing the material and sintering program or the type of starch. Figures 1 and 2 show SEM images of P53A0.20, P58A0.20, P68A0.22, P75A0.22, P71A0.26, P71A0.43, and P82A0.51 before and after soaking in SBF for various periods. There are no closed pores on the surface of a fractured surface. Thus, on the fractured surfaces before soaking all the porous specimens have an open-pore structure with bimodal distributions having pore-size peaks at 10–50 μm and 100–300 μm [5]. Spherical particles were formed on part of the surface of P53A0.20 and P71A0.43 after soaking in SBF for 3 days and covered the entire surface after soaking in SBF for 7 days. Similarly, spherical particles were formed on part of the surface of P58A0.20 after soaking in SBF for 7 days. No particles formed on the surface of P68A0.22, P75A0.22, P71A0.26, and P82A0.51 even after soaking in SBF in 7 days.

Table 3 Porosity, S.S.A., and sample names of the α-TCP porous specimens

Number	Porosity (%)	S.S.A. (m^2 g^{-1})	Sample name
1	53	0.20	P53A0.20
2	58	0.20	P58A0.20
3	68	0.22	P68A0.22
4	75	0.22	P75A0.22
5	71	0.26	P71A0.26
6	71	0.43	P71A0.43
7	82	0.51	P82A0.51

Figure 3 shows the XRD patterns for P53A0.20, P58A0.20, and P68A0.22 before and after soaking in SBF for various periods. All the peaks in the samples P53A0.20, P58A0.20, and P68A0.22 were assigned to the α-TCP phase before soaking. HAp peaks were detected after soaking P53A0.20 in SBF for 3 days and 7 days and soaking P58A0.20 for 7 days. HAp peaks were not detected for P68A0.22 even after soaking in SBF for 7 days.

Figures 4 and 5 show the changes in the Ca and P concentrations of SBF resulting from immersion of P53A0.20, P58A0.20, P68A0.22, P75A0.22, P71A0.26, P71A0.43, and P82A0.51. Remarkable decreases in Ca and P were observed for P53A0.20, P58A0.20, and P71A0.43. In contrast, the Ca and P concentrations were nearly constant during the soaking of P68A0.22, P75A0.22, P71A0.26, and P82A0.51. The Ca and P concentrations increased within 1 day for P53A0.20, P75A0.22, and P71A0.26.

4 Discussion

P53A0.20, P58A0.20, P68A0.22, and P75A0.22 have almost the same S.S.A. but different porosities. The HAp-forming abilities of specimens with the same S.S.A. increased with decreasing porosity. Furthermore, P68A0.22,

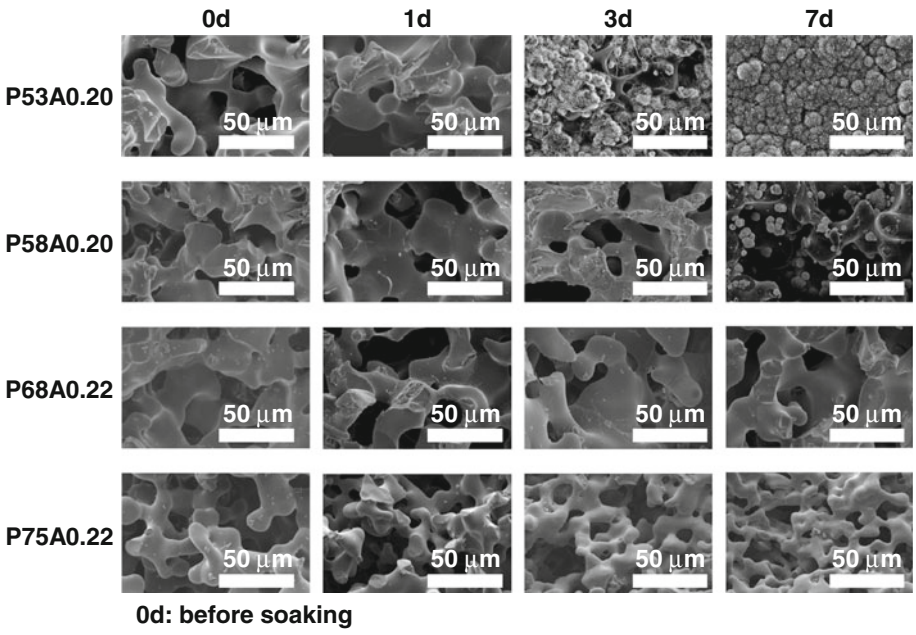

Fig. 1 SEM photographs of P53A0.20, P58A0.20, P68A0.22, and P75A0.22 before and after soaking in SBF

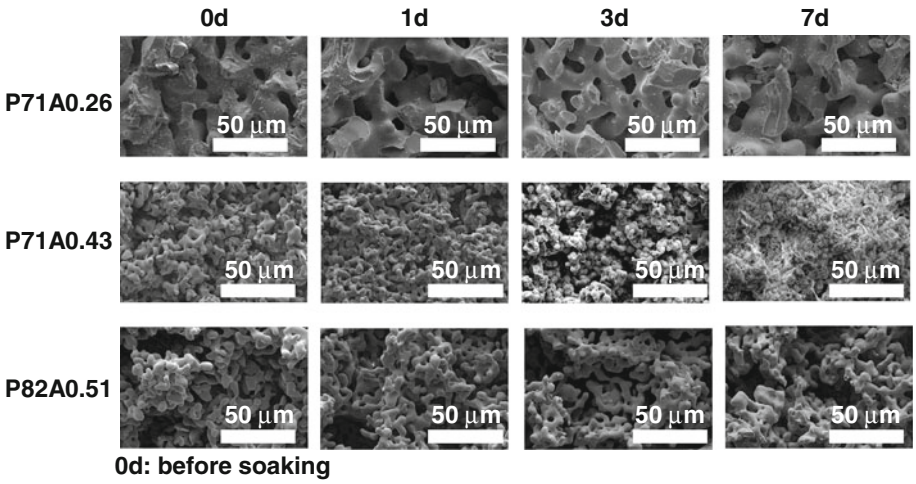

Fig. 2 SEM photographs of P71A0.26, P71A0.43, and P82A0.51 before and after soaking in SBF

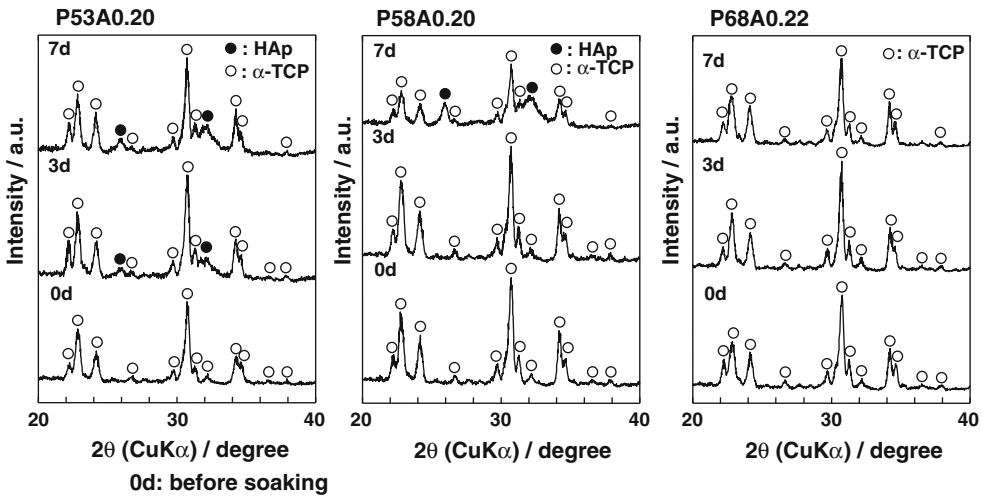

Fig. 3 XRD patterns of specimens before and after soaking in SBF

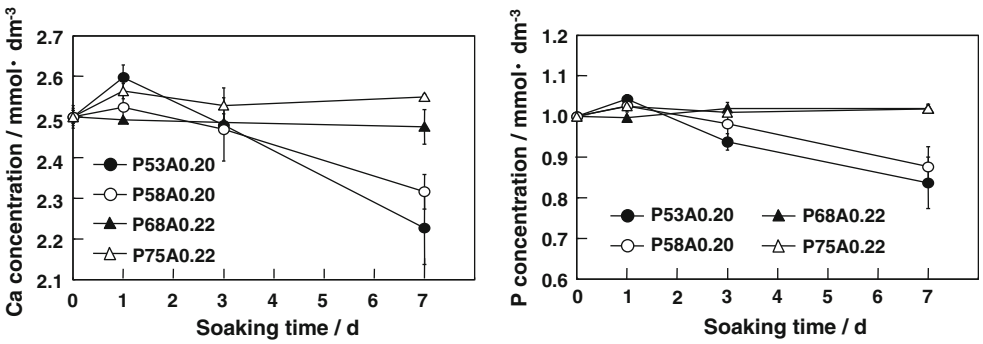

Fig. 4 Changes in Ca and P concentrations in SBF before and after soaking of P53A0.20, P58A0.20, P68A0.22, and P75A0.22

P71A0.26, and P71A0.43 have almost the same porosity but different S.S.A. values. The HAp-forming abilities of specimens with the same porosity increased with increasing S.S.A. Thus, porosity and S.S.A. are important factors for the HAp-forming ability of α-TCP ceramics. However, HAp was not formed on P82A0.51 although it had the largest S.S.A. of all the specimens. The SBF is estimated to be unsaturated with respect to α-TCP and supersaturated with respect to β-TCP [13]. α-TCP may dissolve in SBF.

The initial increase in Ca and P concentrations for P53A0.20, P75A0.22, and P71A0.26 might be caused by debris as well as dissolution of α-TCP. However, these factors did not affect the HAp-formation of α-TCP ceramics. The surface area of the specimen is important for

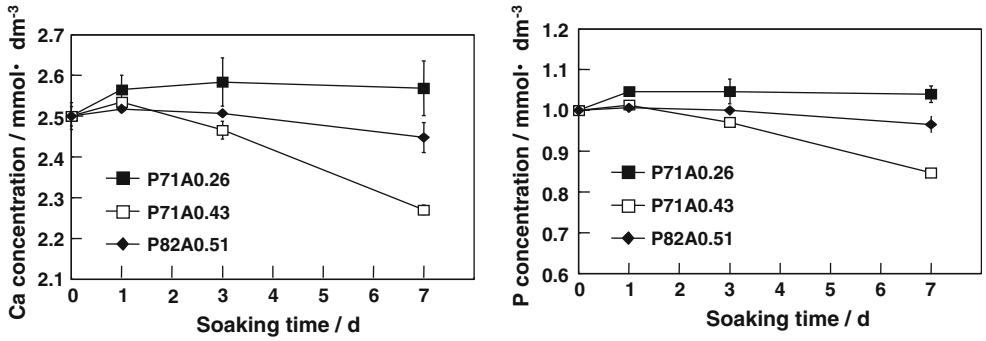

Fig. 5 Changes in Ca and P concentrations in SBF before and after soaking of P71A0.26, P71A0.43, and P82A0.51

the dissolution of α-TCP porous specimens. The dissolution of α-TCP should increase the degree of supersaturation of the surrounding fluid with respect to HAp.

Although P82A0.51 has the largest surface area per unit mass, its surface area per unit volume may be smaller because it has large porosity. The surface area per unit volume depends not only on S.S.A. but also on the porosity. Therefore, we calculated the surface area per unit volume of the specimens. Table 4 shows this area and the HAp-formation of the porous specimens. P53A0.20, P58A0.20, P68A0.22, and P75A0.22 have almost the same surface area per unit mass, but they have different surface areas per unit volume because they have different porosities. The HAp-forming abilities of P53A0.20, P58A0.20, P68A0.22, P75A0.22, P71A0.26, and P71A0.43 increase with increasing surface area per unit volume. However, we can see that although P53A0.20 and P82A0.51 have the same surface area per unit volume, their HAp-forming ability is different. These two specimens have different porosities.

The volume of SBF impregnated in a porous body changes with the porosity of the specimen. An α-TCP porous body may dissolve in SBF impregnated into a porous body at an early stage. The volume of SBF impregnated into a porous body may increase the supersaturation with respect to HAp. Therefore, we calculated the surface area per unit pore volume of the specimens. This value can be obtained by dividing the surface area per unit volume by the pore volume per unit volume. Table 5 shows this area and the HAp-forming ability of the specimens. HAp-formation increased with increasing surface area per unit pore volume.

The high HAp-forming ability of P53A0.20 and P71A0.43 may be the result of the large surface area per unit pore volume of these specimens, which increases the supersaturation of the surrounding fluid with respect to HAp. The surface area per unit pore volume increases with increasing surface area per unit mass and decreasing porosity. Therefore, the HAp-forming ability of porous α-TCP sintered materials could be controlled by the microstructure and depends on the surface area per unit mass and the porosity.

5 Conclusions

The HAp-forming ability of porous α-TCP ceramics increases with surface area per unit pore volume of the specimens when they have similar pore structures. A large surface area per unit pore volume leads to an increased local concentration of Ca^{2+} in the SBF impregnated into the porous body, increasing the degree of supersaturation with respect to HAp. Thus, the microstructure of the specimens is significant for determining both the bioresorbability and the HAp-formation.

Table 4 Surface areas per volume and HAp-forming ability of porous specimens

Sample name	Surface area per volume (m^2 m^{-3})	HAp-forming ability
P53A0.20	0.26	Formed within 3 days
P58A0.20	0.24	Formed within 7 days
P68A0.22	0.20	Not formed within 7 days
P75A0.22	0.16	Not formed within 7 days
P71A0.26	0.22	Not formed within 7 days
P71A0.43	0.36	Formed within 3 days
P82A0.51	0.27	Not formed within 7 days

Table 5 Surface areas per unit pore volume and HAp-forming ability of specimens

Sample name	Surface area per unit pore volume (m^2 m^{-3})	HAp-forming ability
P53A0.20	0.50	Formed within 3 days
P58A0.20	0.42	Formed within 7 days
P68A0.22	0.30	Not formed within 7 days
P75A0.22	0.21	Not formed within 7 days
P71A0.26	0.32	Not formed within 7 days
P71A0.43	0.50	Formed within 3 days
P82A0.51	0.32	Not formed within 7 days

References

1. Rejda BV, Peelen JG, DE KGroot. Tri-calcium phosphate as a bone substitute. J Bioeng. 1977;1:93–7.
2. Metsger DS, Driskell TD, Paulsrud JR. Tricalcium phosphate ceramic—a resorbable bone implant: review and current status. J Am Dent Assoc. 1982;105:1035–8.
3. Fujishiro Y, Takahashi K, Sato T. Preparation and compressive strength of alpha-tricalcium phosphate/gelatin gel composite cement. J Biomed Mater Res. 2001;54:525–30.
4. Yuan H, Bruijin JDDE, Li Y, Feng J, Yang Z, Groot KDE, et al. Bone formation induced by calcium phosphate ceramics in soft tissue of dogs: a comparative study between porous α-TCP and β-TCP. J Mater Sci: Mater Med. 2001;12:7–13.
5. Kitamura M, Ohtsuki C, Ogata S, Kamitakahara M, Tanihara M. Microstructure and bioresorbable properties of α-TCP ceramic porous body fabricated by direct casting method. Mater Trans. 2004;45:983–8.
6. Kitamura M, Ohtsuki C, Iwasaki H, Ogata S, Tanihara M, Miyazaki T. The controlled resorption of porous α-tricalcium phosphate using a hydroxypropylcellulose coating. J Mater Sci: Mater Med. 2004;15:1153–8.
7. Kokubo T, Kushitani H, Sakka S, Kitsugi T, Yamamuro T. Solutions able to reproduce in vivo surface-structure changes in bioactive glass-ceramic A-W. J Biomed Mater Res. 1990;24:721–34.
8. Cho SB, Nakanishi K, Kokubo T, Soga N, Ohtsuki C, Nakamura T, et al. Dependence of apatite formation on silica gel on its structure: effect of heat treatment. J Am Ceram Soc. 1995; 78:1769–74.
9. Ohtsuki C, Aoki Y, Kokubo T, Bando Y, Neo M, Nakmura T. Transmission electron microscopic observation of glass-ceramic A-W and apatite layer formed on its surface in a simulated body fluid. J Ceram Soc Jpn. 1995;103:449–54.
10. Kokubo T, Takadama H. How useful is SBF in predicting in vivo bone bioactivity? Biomaterials. 2006;27:2907–15.
11. Uchino T, Ohtsuki C, Kamitakahara M, Tanihara M, Miyazaki T. Apatite formation behavior on tricalcium phosphate (TCP) porous body in a simulated body fluid. Key Eng Mater. 2006; 309–311:251–4.
12. Elliot JC. Structure and chemistry of the apatites and other calcium orthophosphates. Amsterdam: Elsevier; 1994. p. 34.
13. Ohtsuki C, Tanihara M, Miyazaki T, Ogata S. Hand book of organic-inorganic hybrid materials and nanocomposites. Valencia, CA: American Scientific Publishers; 2003. p. 265–93.